

# Dispersion of carbon nanotubes in melt compounded polypropylene based composites investigated by THz spectroscopy

R. Casini,<sup>1</sup> G. Papari,<sup>1</sup> A. Andreone,<sup>1,2,\*</sup> D. Marrazzo,<sup>3</sup> A. Patti,<sup>3</sup> and P. Russo<sup>4</sup>

<sup>1</sup> Physics Department, University of Naples "Federico II", Naples, Italy

<sup>2</sup> Institute SPIN, National Research Council, UOS Naples, Italy

<sup>3</sup> Department of Chemical, Materials Engineering and Industrial Production, University of Naples "Federico II", Naples, Italy

<sup>4</sup> Institute for Polymers, Composites and Biomaterials, National Research Council, Pozzuoli (Na), Italy

\*andreone@umina.it

**Abstract:** We investigate the use of Terahertz (THz) Time Domain Spectroscopy (TDS) as a tool for the measurement of the index dispersion of multi-walled carbon nanotubes (MWCNT) in polypropylene (PP) based composites. Samples containing 0.5% by volume concentration of non-functionalized and functionalized carbon nanotubes are prepared by melt compounding technology. Results indicate that the THz response of the investigated nanocomposites is strongly dependent on the kind of nanotube functionalization, which in turn impacts on the level of dispersion inside the polymer matrix. We show that specific dielectric parameters such as the refractive index and the absorption coefficient measured by THz spectroscopy can be both correlated to the index of dispersion as estimated using conventional optical microscopy.

©2015 Optical Society of America

**OCIS codes:** (300.6495) Spectroscopy, terahertz; (160.5470) Polymers; (160.4236) Nanomaterials.

---

## References and links

1. L. Vaisman, H. D. Wagner, and G. Marom, "The role of surfactants in dispersion of carbon nanotubes," *Adv. Colloid Interface Sci.* **128-130**, 37–46 (2006).
2. B. Yalcin and M. Cakmak, "The role of plasticizer on the exfoliation and dispersion and fracture behavior of clay particles in PVC matrix: a comprehensive morphological study," *Polymer (Guildf.)* **45**(19), 6623–6638 (2004).
3. P.-C. Ma, N. A. Siddiqui, G. Marom, and J.-K. Kim, "Dispersion and functionalization of carbon nanotubes for polymer-based nanocomposites: a review," *Compos., Part A Appl. Sci. Manuf.* **41**(10), 1345–1367 (2010).
4. M. Pokrass, Z. Burshtein, R. Gvishi, and M. Nathan, "Saturable absorption of multi-walled carbon nanotubes/hybrid-glass composites," *Opt. Mater. Express* **2**(6), 825–838 (2012).
5. X.-L. Zhang, Z.-B. Liu, X. Zhao, X.-Q. Yan, X.-C. Li, and J.-G. Tian, "Optical limiting effect and ultrafast saturable absorption in a solid PMMA composite containing porphyrin-covalently functionalized multi-walled carbon nanotubes," *Opt. Express* **21**(21), 25277–25284 (2013).
6. B. Xu, M. Omura, M. Takiguchi, A. Martinez, T. Ishigure, S. Yamashita, and T. Kuga, "Carbon nanotube/polymer composite coated tapered fiber for four wave mixing based wavelength conversion," *Opt. Express* **21**(3), 3651–3657 (2013).
7. A. Martinez, S. Uchida, Y.-W. Song, T. Ishigure, and S. Yamashita, "Fabrication of Carbon nanotube poly-methyl-methacrylate composites for nonlinear photonic devices," *Opt. Express* **16**(15), 11337–11343 (2008).
8. T. Schibli, K. Minoshima, H. Kataura, E. Itoga, N. Minami, S. Kazaoui, K. Miyashita, M. Tokumoto, and Y. Sakakibara, "Ultrashort pulse-generation by saturable absorber mirrors based on polymer-embedded carbon nanotubes," *Opt. Express* **13**(20), 8025–8031 (2005).
9. G. Lamura, A. Andreone, Y. Yang, P. Barbara, B. Vigolo, C. Herold, J.-F. Mareche, P. Lagrange, M. Cazayous, A. Sacuto, M. Passacantando, F. Bussolotti, and M. Nardone, "High-crystalline single- and double-walled carbon nanotube mats grown by chemical vapor deposition," *J. Phys. Chem. C* **111**(42), 15154–15159 (2007).
10. S. Pegel, P. Potschke, G. Petzold, I. Alig, S. M. Dudkin, and D. Lellinger, "Dispersion, agglomeration, and network formation of multiwalled carbon nanotubes in polycarbonate melts," *Polymer (Guildf.)* **49**(4), 974–984 (2008).

11. A. Battisti, A. A. Skordos, and I. K. Partridge, "Monitoring dispersion of carbon nanotubes in a thermosetting polyester resin," *Compos. Sci. Technol.* **69**(10), 1516–1520 (2009).
12. N. G. Sahoo, S. Rana, J. W. Cho, L. Li, and S. H. Chan, "Polymer nanocomposites based on functionalized carbon nanotubes," *Prog. Polym. Sci.* **35**(7), 837–867 (2010).
13. A. Durmus, A. Kasgoz, and C. W. Macosko, "Linear low density polyethylene (LLDPE)/clay nanocomposites. Part I: structural characterization and quantifying clay dispersion by melt rheology," *Polymer (Guildf.)* **48**(15), 4492–4502 (2007).
14. A. B. Morgan and J. W. Gilman, "Characterization of polymer-layered silicate (clay) nanocomposites by transmission electron microscopy and X-ray diffraction: a comparative study," *J. Appl. Polym. Sci.* **87**(8), 1329–1338 (2003).
15. E. J. Garboczi, K. A. Snyder, J. F. Douglas, and M. F. Thorpe, "Geometrical percolation threshold of overlapping ellipsoids," *Phys. Rev. E Stat. Phys. Plasmas Fluids Relat. Interdiscip. Topics* **52**(1), 819–828 (1995).
16. P. Russo, A. Patti, and D. Acierno, "Effects of chemical functionalization of multi wall carbon nanotubes on the heat transport behaviour of polypropylene based nanocomposites," *AIP Conf. Proc.* **1599**, 406 (2014).
17. W. Bauhofer and J. Z. Kovacs, "A review and analysis of electrical percolation in carbon nanotube polymer composites," *Compos. Sci. Technol.* **69**(10), 1486–1498 (2009).
18. A. Combessis, C. Mazel, M. Maugin, and L. Flandin, "Optical density as a probe of carbon nanotubes dispersion in polymers," *J. Appl. Polym. Sci.* **130**(3), 1778–1786 (2013).
19. S. Wietzke, C. Jansen, M. Reuter, T. Jung, D. Kraft, S. Chatterjee, B. M. Fischer, and M. Koch, "Terahertz spectroscopy on polymers: a review of morphological studies," *J. Mol. Struct.* **1006**(1-3), 41–51 (2011).
20. S. Wietzke, C. Jansen, T. Jung, M. Reuter, B. Baudrit, M. Bastian, S. Chatterjee, and M. Koch, "Terahertz time-domain spectroscopy as a tool to monitor the glass transition in polymers," *Opt. Express* **17**(21), 19006–19014 (2009).
21. N. Krumbholz, T. Hochrein, N. Vieweg, T. Hasek, K. Kretschmer, M. Bastian, M. Mikulics, and M. Koch, "Monitoring polymeric compounding processes inline with THz time-domain spectroscopy," *Polym. Test.* **28**(1), 30–35 (2009).
22. F. Rutz, M. Koch, S. Khare, M. Moneke, H. Richter, and U. Ewert, "Terahertz quality control of polymeric compounds," *Int. J. Infrared Millimeter Waves* **27**(4), 547–556 (2006).
23. D. Akbar and H. Altan, "Characterization of polypropylene treated under dual-RF plasma using Terahertz time-domain spectroscopy," *J. Mater. Sci.* **48**(23), 8209–8214 (2013).
24. B. M. Fischer, S. Wietzke, M. Reuter, O. Peters, R. Gente, C. Jansen, N. Vieweg, and M. Koch, "Investigating material characteristics and morphology of polymers using Terahertz technology," *IEEE Trans. THz Sci. Technol.* **3**(3), 259–268 (2013).
25. O. Peters, S. F. Busch, B. M. Fischer, and M. Koch, "Determination of the carbon nanotube concentration and homogeneity in resin films by THz spectroscopy and imaging," *J. Infrared, Millimeter, and THz Waves* **33**, 1221–1226 (2012).
26. S. Wietzke, C. Jansen, F. Rutz, D. M. Mittleman, and M. Koch, "Determination of additive content in polymeric compounds with terahertz time-domain spectroscopy," *Polym. Test.* **26**(5), 614–618 (2007).
27. N. Krumbholz, T. Hochrein, N. Vieweg, I. Radovanovic, I. Pupeza, M. Schubert, K. Kretschmer, and M. Koch, "Degree of dispersion of polymeric compounds determined with terahertz time-domain spectroscopy," *Polym. Eng. Sci.* **51**(1), 109–116 (2011).
28. B. Krause, P. Pötschke, and L. Häußler, "Influence of small scale melt mixing conditions on electrical resistivity of carbon nanotube-polyamide composites," *Compos. Sci. Technol.* **69**(10), 1505–1515 (2009).
29. S. Pegel, PhD Thesis, Material Science Technical University Dresden – Dresden (2010).
30. M. Bernier, F. Garet, and J. L. Coutaz, "Precise determination of the refractive index of sample showing low transmission bands by THz Time Domain Spectroscopy," *IEEE Trans. THz Sci. Technol.* **3**(3), 295–301 (2013).
31. Y. S. Jin, G. J. Kim, and S. G. Jeon, "Terahertz dielectric properties of polymers," *J. Korean Phys. Soc.* **49**, 513–517 (2006).
32. I. Pupeza, R. Wilk, and M. Koch, "Highly accurate optical material parameter determination with THz time-domain spectroscopy," *Opt. Express* **15**(7), 4335–4350 (2007).
33. L. Liu, A. Das, and C. M. Megaridis, "Terahertz shielding of carbon nanomaterials and their composites. A review and applications," *Carbon* **69**, 1–16 (2014).

---

## 1. Introduction

Polymer nanocomposites (PNCs), widely cited in the literature since the early '90s, still attract a remarkable interest from the academic and industrial research. PNCs in fact display unique functional properties that can be acquired with relatively small amounts of fillers in comparison with traditional microcomposites. Nevertheless, the diffusion of materials containing nanofillers remains very limited, mainly because of technological difficulties to reproduce at an industrial level a filler dispersion similar to that obtained on a laboratory scale. This drawback is essentially related to interactions among the dispersed particles that

reduce the specific surface area of the interface. The problem has been addressed by various approaches, and a variety of solutions to prevent particle aggregation have been proposed, including the use of auxiliaries such as surfactants [1] and plasticizers [2] or chemical functionalization of the filler-matrix interface [3]. Among nanofillers, carbon nanotubes (CNTs) are extremely promising since they combine extremely high stiffness, large electrical and thermal conductivity, together with high aspect ratios which may give rise to new materials with interesting potential uses in different industrial fields such as electronic and car industries. As far as photonic applications are concerned, CNTs in a solid composite represent an attractive material due to their nonlinear optical properties, such as large saturable absorption [4] and high third order nonlinearity [5]. In the past few years, there have been plenty of reports on the fabrication of CNT based compounds from which complex nonlinear optical devices (such as fibers for wavelength conversion [6], or waveguides [7] and saturable absorbers [8] for passive mode locking in solid-state lasers) can be realized.

Carbon nanotubes are mainly produced by chemical vapor deposition (CVD) and are generally available as highly entangled and agglomerated structures [9]. They are very difficult to disperse in polymer resins, especially using the melt compounding technology. This is a very attractive mixing process from both industrial and safety point of view, with respect to other ones such as in situ polymerization, solvent mixing and so on. In this regard, many studies have been carried out to investigate the mechanisms of dispersion of CNTs in both thermoplastic and thermosetting polymer matrices [10, 11]. In general, for PNCs the influence of process conditions, filler content, matrix viscosity, interfacial nature and aspect ratio on the so-called percolation thresholds and ultimate properties have been extensively considered [12]. Qualitative information about agglomerates formed during inappropriate mixing is generally drawn from rheological measurements [13], microscopic observations or using X-rays diffraction tests [14]. These analyses are intrinsically limited and do not allow a complete characterization of the complex three-dimensional structures of the CNT aggregates.

Previous investigations have clearly evidenced that, despite the outstanding potential of carbon nanotubes, there are still many difficulties related to their dispersion. Conventional processing technologies cause random disposition as well as poor alignment of the nanofillers in the hosting matrix. Significant ultimate functional benefits can be only achieved by inserting adequate CNT contents, usually above the so-called theoretical percolation threshold [15]. In [16], Russo *et al.* reported that a relevant increase of the thermal conductivity of polypropylene is verified above a threshold of 0.5% in volume (1% by weight) of carbon nanotubes. The number nicely matches the electrical percolation threshold (ranging from 0.1 to 3% by weight CNT [17]), although an exact value cannot be given in this case since it is very much dependent on the kind of carbon nanotubes, viscosity and wettability of the hosting matrix polymer, and degree of dispersion. Many studies are currently attempting to quantitatively estimate the index of dispersion  $D$  as a function of filler content and typology [18]. However, these analytical approaches are usually difficult and time consuming to be applied systematically, besides being mostly off-line.

Terahertz Time Domain Spectroscopy has been widely employed as a characterization tool for a wide variety of materials, including ceramics, semiconductors and superconductors, and polymeric compounds. TDS being a coherent technique, refraction and absorption as a function of frequency can be directly derived from a comparison of the phase and amplitude spectrum of the pulses transmitted through the samples relatively to the reference pulse. On the contrary, non-coherent spectroscopy systems such as Fourier Transform-Infrared Spectroscopy (FTIR) don't enable direct calculation of material parameters, and Kramers-Kronig algorithm must be used to retrieve refractive index information. As far as polymers are concerned, THz-TDS has been recently used for morphological studies [19], to monitor glass transitions [20] and compounding processes [21], for quality control [22], or simply for material characterization [23, 24]. More specific studies have been focused on the properties of polymeric compounds containing different types of additives. In [25], Peters *et al.*

investigated the concentration of multi-walled carbon nanotubes embedded in a resin matrix, showing that inhomogeneities can be detected using THz imaging. In [26], Wietzke *et al.* drew the same conclusion analyzing different additives and compounds. In [27], Krumbholtz *et al.* found that in polymer-based compounds containing wooden fibers THz spectroscopy measurements allows discriminating among samples with different degree of dispersion. In all cases, the importance of a fast, reliable and non-destructive method to detect the level of sample homogeneity and nanofillers dispersion in polymeric composites was clearly pointed out.

The main aim and the interest of the present work is to show that THz-TDS can be exploited also to correlate the optically determined index  $D$  with specific spectroscopic parameters, refractive index  $n$  and absorption coefficient  $\alpha$ , as derived by the high frequency measurements. Nanocomposites based on polypropylene and containing multi-walled carbon nanotubes for concentrations above the so-called theoretical percolation threshold (0.5% in vol.) and different surface features have been prepared. Samples have been systematically analyzed with both the conventional optical microscopy and time domain spectroscopy approach. Results and considerations presented in our work allow to appreciate the versatility of this alternative technique, already widely validated for other applications, to acquire fast information on the quality of polymer nanocomposites suitable for the development of optical devices.

## 2. Experimental methods

### 2.1 Materials and sample preparation

A commercial polypropylene resin Monsten MA524 (MFI 24.0 g/10min @230 °C, 2.16 Kg), supplied by UNIPETROL RPA, was modified by inclusion of MWCNTs (average length < 1  $\mu$ m, average diameter: 9.5 nm, true density: 1.94 g/ml), supplied by Nanocyl S.A. Three types of thin multi-wall carbon nanotubes were produced via the catalytic CVD process and then purified to greater than 95% carbon to produce the 3150 grade (bulk density 100 g/l). This grade is then functionalized with carboxyl (-COOH) and amino (-NH<sub>2</sub>) groups to produce the 3151 (bulk density 250 g/l) and 3152 (bulk density 150 g/l) grades respectively.

The nanocomposites were prepared by melt blending the PP matrix, as received from the manufacturer, with carbon nanotubes in a Brabender mixer Plastograph ECbatch, setting a rotation speed of 60 rpm and a temperature of 190 °C. For each batch, 45 g of polypropylene resin was fed into the mixing chamber and processed for 2 minutes to melt the whole polymer. At this point, MWCNTs with a concentration of 0.5% by volume were added with continuous mixing for additional 5 minutes. A systematic evaluation of the content of filler by thermo-gravimetric analysis confirmed a remarkable agreement between the nominal and effective values. Samples were obtained by compression molding with a Lab Tech Engineering hydraulic press, setting a pressure of 70 bar and a temperature of 210 °C.

### 2.2 Optical microscopy

For each nanocomposite, 10 slices with an average thickness of about 7 microns were obtained by using a Leica CM1850 microtome at room temperature and analyzed by optical microscope Olympus BX53. Slices were taken from different regions of the same compression molded sample in order to check the achieved level of uniformity in terms of MWCNT agglomerate size distribution. For each slice, the dispersion index  $D$  of the nanofillers was evaluated according to the following equation [28]:

$$D = \left( 1 - f \frac{A/A_0}{V} \right) \cup 100\% \quad (1)$$

where  $A$  and  $A_0$  represent the area occupied by agglomerates and the total investigated area, respectively;  $V$  is the carbon nanotube volume fraction, and  $f$  is a factor related to the density

of MWCNT agglomerates and measured according to the procedure reported in [29]. In particular, for each observed section, a particle analysis was performed using the Java-based free software ImageJ (National Institutes of Health, United States) and neglecting agglomerates with diameters smaller than 5  $\mu\text{m}$ .

### 2.3 Terahertz spectroscopy

A customised THz-TDS system (EKSPLA, Lithuania), based on a 1064 nm fiber laser with 120 fs pulse width and 60 MHz repetition rate, is used for the measurements. In the standard setup, the laser output is split in 2 beams. Pump beam generates an electromagnetic (e.m.) transient (THz pulse,  $\approx\text{ps}$ ) through the excitation of a low-temperature grown GaBiAs-based photoconductive antenna (PCA) emitter, whereas the probe beam is used to detect the THz pulse using a similar PCA receiver. A mechanical optical line is used to control the delay between probe and pump beams. This method of detection provides the waveform, that is the electric field amplitude of the THz pulse as a function of the timing difference. Two hyper-hemispherical high resistivity silicon lenses collect and focus emitted and detected radiation from PCAs. Measurements are carried out on freestanding samples placed along the beam path in the focus of two off-axis parabolic mirrors. The spot diameter is about 2 mm. Thickness of bulk samples for the THz measurements has been set to a minimum (1.4 mm), in the attempt to enhance as much as possible the THz transmission band [30]. All measurements are performed in a nitrogen-controlled atmosphere, to reduce or eliminate in the frequency spectra the water absorption lines caused by signal transmission in air. By using TDS we can compare the dielectric properties of polypropylene-based composites loaded using MWCNTs in the frequency band 0.3 – 1.4 THz and with a maximum dynamic range of about 60 dB, strongly dependent on the transmittance properties of each sample.

### 3. Results and discussion

Image analysis, carried out on several slices of material for each sample, shows that a satisfactory MWCNT aggregate size distribution is always achieved under the applied processing conditions. Figure 1 displays the representative light microscopy images of polypropylene compounds containing 0.5% in volume for each kind of carbon nanotubes herein considered: non-functionalized, functionalized with amino groups ( $-\text{NH}_2$ ), functionalized with carboxyl groups ( $-\text{COOH}$ ).

Optical micrographs highlight the diverse typology of agglomerate dispersion in the samples under investigation. These differences are clearly reflected in the dispersion index calculated according to Eq. (1) and reported in Table 1 for each system.

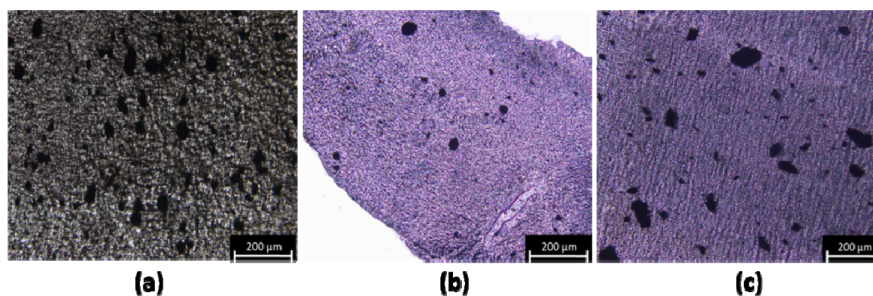


Fig. 1. Optical micrographs illustrating the state of agglomerate dispersion of nanocomposites with different type of MWCNTs: non-functionalized (a), functionalized with amino groups (b) and functionalized with carboxyl groups (c).

**Table 1. Packing density  $f$  and dispersion index  $D$  for the nanocomposites with different type of MWCNTs.**

	Nanocyl 3150	Nanocyl 3151	Nanocyl 3152
Functionalization	None	-COOH	-NH <sub>2</sub>
Packing density $f^*$	0.025	0.029	0.025
Dispersion index $D$ (%)	60	86	86

\* Determined as reported by Pegel [29]

In particular, evaluations highlight that the worst dispersion index  $D$  occurs in presence of non-functionalized carbon nanotubes, whereas for both types of surface modified nanotubes the same parameter increases and reaches a similar value.

The number of agglomerates, instead, vary from 60 counts/mm<sup>2</sup> for compounds filled with carboxyl-modified carbon nanotubes up to 320 and 470 counts/mm<sup>2</sup> for systems containing the same amount of amino-modified and pristine carbon nanotubes, respectively. In other words, although the dispersion of carbon nanotubes seems to be favored at the same extent in presence of the two considered surface modified carbon nanotubes, the type of functional group apparently influence the number of remaining MWCNT agglomerates and their size distribution. This is presumably related to expected differences in terms of filler-matrix interactions and steric hindrance of functional groups present on the surface of the filler. Such a conjecture has been further supported by the software-based image analysis, which allows obtaining the size distribution of detected aggregates for each type of MWCNT (Figs. 2(a)–2(c)). Graphs highlight that non-functionalized MWCNTs give rise to a higher number of agglomerates with an average size (equivalent diameter) larger than functionalized ones, reducing the dispersion index of melted compounds.

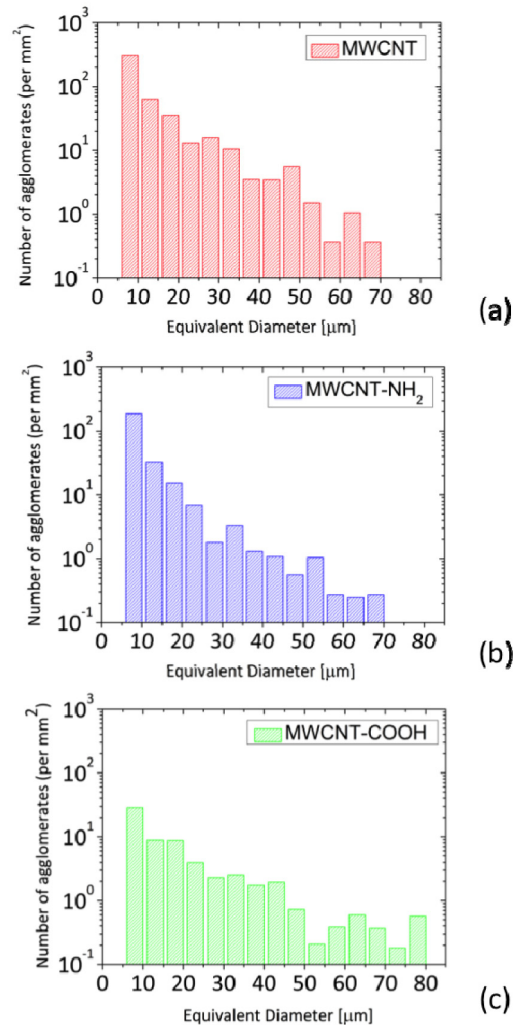


Fig. 2. Size distribution of MWCNT agglomerates in nanocomposites with different functionalized filler: non-functionalized (a), functionalized with amino groups (b), and functionalized with carboxyl groups (c).

A terahertz pulse is measured without any sample placed in the beam path, and used as a reference. This makes unnecessary complicate and laborious calibrations of the measuring system. The hosting polypropylene resin, being a non-polar polymer, in absence of any filler is almost transparent to the electromagnetic radiation in the THz band [31] and can be easily characterized using the TDS in the overall frequency range of operation (0.5 – 3 THz). The insertion of conductive MWCNTs in this resin increases THz absorption, with a strong reduction of the Signal-to-Noise Ratio (SNR), making possible reliable measurements up to 1.4 THz only.

Figure 3 shows the measurement of the reference signal (black solid line) compared with the same signal (vertically shifted, for the sake of clarity) passing respectively through the polypropylene matrix only and through samples containing both non- and functionalized MWCNTs. Actually, the THz pulse transmitted from the sample fabricated using the neat PP

resin doesn't show a noticeable change in the signal intensity and shape with respect to the reference. Polymer nanocomposites instead show a significant reduction in signal amplitude relatively to the reference waveform, due to the absorption and reflection mechanisms produced by the presence of CNT fillers. Furthermore, for all samples the observed time delay is caused from the higher refractive index they have in comparison with air (nitrogen).

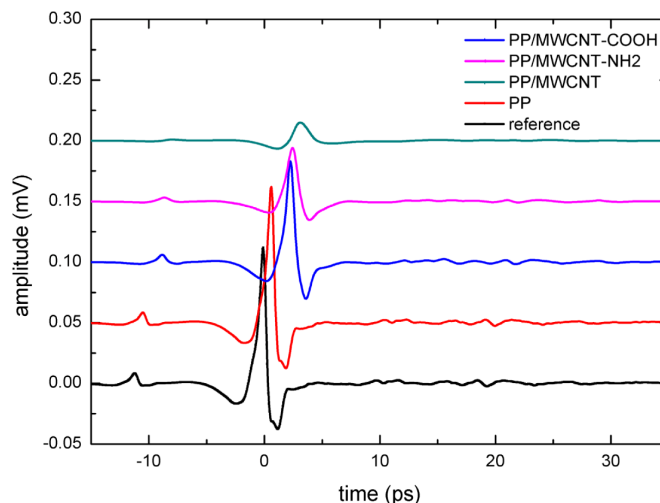


Fig. 3. THz reference signal vs time (black line) compared with the PP matrix only (red line), and with the nanocomposites loaded with MWCNTs, non-functionalized (green line) and functionalized with  $\text{NH}_2$  (cyan line) and  $\text{COOH}$  (blue line) respectively. For the sake of clarity, signals are vertically shifted by a constant value (0.05 arb. u.)

Related frequency spectra in Fig. 4 using Fast Fourier Transform (FFT) confirm that the different degree of MWCNT functionalization clearly produces a relevant change in the sample behavior. In all samples, THz transmission strongly decreases with frequency. In polymer nanocomposites the normalized signal transmission is also strongly reduced, and this is more and more evident increasing the THz frequency. On the contrary, data for the sample based on the pure polypropylene are remarkably similar to the behavior shown by the reference signal (not displayed here), confirming the high transparency of the PP matrix. The worst case results to be for the sample having carbon nanotubes that are not functionalized at all, where the power absorption is order of magnitude larger than for the other samples.

To be more quantitative, we can compare the refractive index  $n$  and absorption coefficient  $\alpha$  of the polypropylene sample only with nanocomposites containing MWCNTs, in order to understand if the THz technique can detect and diversify the different typology of carbon nanotubes and relate it to the dispersion index. Results on both  $n$  and  $\alpha$  vs frequency show that the polymer matrix acts almost as an “invisible” background medium, allowing to easily characterize the embedded MWCNTs only. For the data analysis we use commercial software, TeraLizer<sup>TM</sup>, where a proprietary iterative algorithm [32] is exploited to extract with high accuracy the material parameters from the frequency spectrum. We compare the sample pulse (sample in the THz beam) with the reference pulse (empty THz-TDS system). The measured transfer function is the ratio of the corresponding Fourier spectra. For the parameters evaluation, the software minimizes the difference between the measured and the theoretical transfer functions. In our case, the optimum thickness best fitting the data is  $1.40 \pm 0.05$  mm, perfectly matching the measured sample thickness.



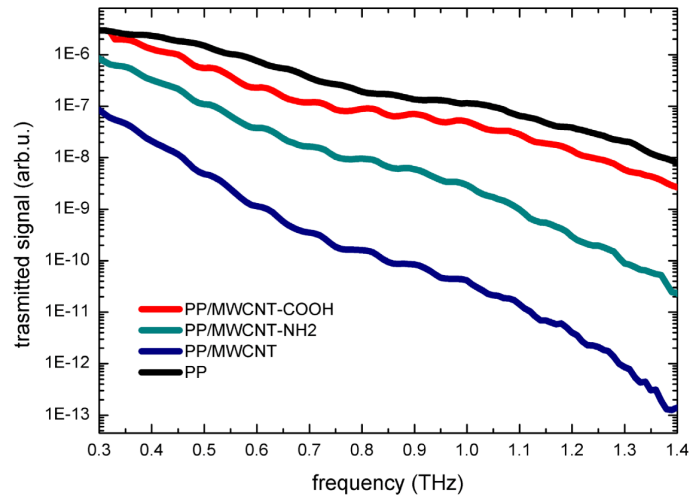


Fig. 4. Transmitted signal calculated from FFT for the neat PP matrix (black line) and for the nanocomposites loaded with MWCNTs, non-functionalized (blue line) and functionalized with  $\text{NH}_2$  (cyan line) and  $\text{COOH}$  (red line) respectively.

Figure 5 displays the refractive index of the nanocomposites containing MWCNTs with different functionalization as a function of frequency. At the highest frequencies (above 1 THz), the small SNR value makes difficult spectrum analysis, rendering data comparison less reliable. The corresponding behavior for the polypropylene matrix is shown for comparison.

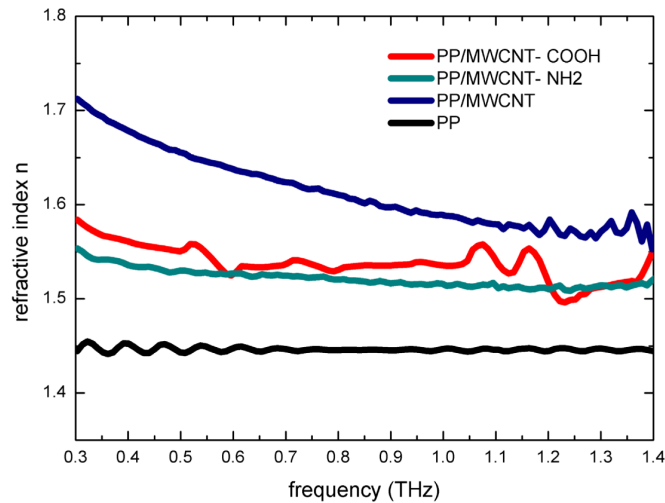


Fig. 5. Refractive index  $n$  as a function of frequency for the neat PP matrix and for the nanocomposites loaded with MWCNTs having different functionalization.

One can see that the  $n$  value for the sample loaded with MWCNTs that are not functionalized is always higher than in the case of functionalized samples at every investigated frequency. The smallest values are found for the neat polymer matrix. In this last case, as expected, the refractive index of the sample is nearly constant in the overall range because of its non-polar nature and the absence of any resonant behavior in this frequency

band [19]. On the other hand,  $n$  in nanocomposites slightly decreases with frequency, this behavior being more evident for the non-functionalized sample.

The frequency behavior of the absorption coefficient is displayed in Fig. 6.

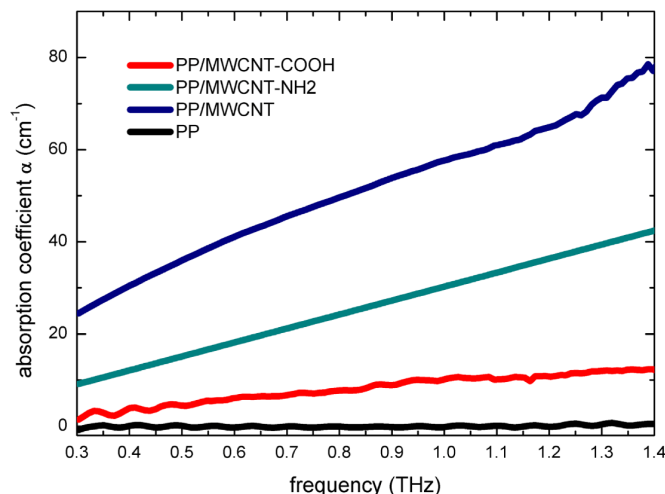


Fig. 6. Absorption coefficient  $\alpha$  as a function of frequency for the neat PP matrix and for the nanocomposites loaded with MWCNTs having different functionalization.

In nanocomposites,  $\alpha$  always increases as a function of frequency with a linear or sub-linear term. This is in agreement with previous findings [25]. In terms of absolute values, the insertion of carbon nanotubes in the polymer matrix produces a significant rise of the absorbed and scattered energy inside each nanocomposite, which is however strongly dependent on the different degree of MWCNTs functionalization. The lowest  $\alpha$  values are observed for the sample functionalized with carboxyl groups (-COOH), which shows a level of signal attenuation fairly close to the sample without any filler content. The largest increase instead is observed in the case of the sample containing non-functionalized MWCNTs, where the absorption coefficient more than doubles. Here  $\alpha$  well correlates with  $n$  too, since the refractive index is always higher than in functionalized samples, indicating an increased interaction between the medium and the THz wave. The level of absorption for the nanocomposite functionalized with amino groups (-NH<sub>2</sub>) lies somehow in between the two previous cases.

We speculate that several mechanisms can be responsible for the observed behaviors:

- the high number of agglomerates which are present in nanocomposites containing both non-functionalized and amino modified MWCNTs, giving rise to a larger Rayleigh scattering (nicely scaling with frequency) in those samples;
- the oxidation treatment of the MWCNTs that usually removes other carbon impurities, generally improving the filler conductivity. This might partially account for the lower level of absorption observed in samples filled with carboxyl modified MWCNTs with respect to ones containing amino modified MWCNTs [26];
- the MWCNTs functionalization itself, leading to a higher degree of dispersion in the polymer and consequently to a smaller number of agglomerates having dimensions comparable with the wavelength (see Fig. 2). This in turn might reduce the number of significant scattering sources in the frequency region under investigation for the same level of nanofiller content.

The correlation between the dispersion estimated using optical microscopy and the THz wave interaction can be seen in Figs. 7(a) and 7(b), where  $D$  is reported as a function of the refractive index and the absorption coefficient respectively. Data are shown at the operational frequency of 0.5 THz since the SNR value is the highest, however a similar behavior is observed in the full range of investigation.

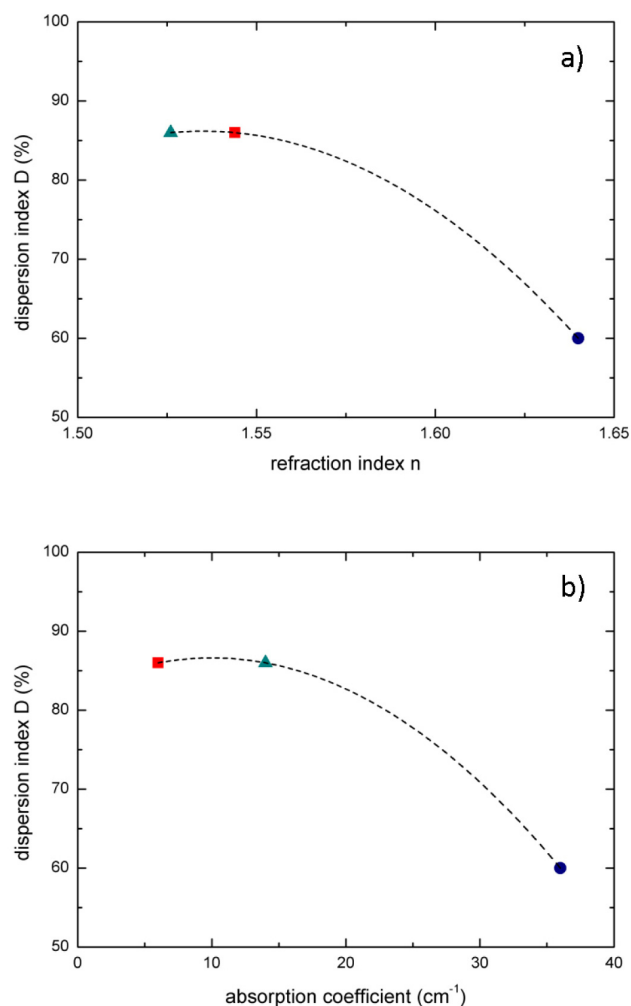


Fig. 7. Plot of the degree of dispersion  $D$  as estimated using optical microscopy vs (a)  $n$  and (b)  $\alpha$  values measured through THz spectroscopy for the nanocomposites loaded with MWCNTs having different functionalization: pristine (full circle), with amino groups (full triangle), with carboxyl groups (full square). The frequency of investigation is 0.5 THz. The dashed curves represent a guide-to-the-eye only.

Functionalized samples with the largest  $D$  values show the smallest  $n$  and  $\alpha$  values, that is the smallest interaction between the medium and the transmitted e.m. wave. Our understanding is therefore that samples where CNTs are well dispersed, namely with a homogeneous distribution of the nanofillers, can be easily distinguished by poorly dispersed samples simply looking at their electromagnetic response in the THz region. On the other hand, since polymeric compounds loaded with CNTs having no functionalization at all show

the highest level of signal absorption, this behavior can be used as a “rule of thumb” and a practical route towards the development of recently proposed carbon based nanocomposites for the electromagnetic interference shielding of THz waves [33].

#### 4. Conclusions

The aim of the present paper was to compare the dispersion index of MWCNTs in the polymer matrix, as evaluated through the optical method, with the analysis carried out using high frequency measurements, in order to understand how different numbers of agglomerates can modify the material dielectric parameters, and to validate the THz Time Domain Spectroscopy as an alternative and reliable non destructive method to measure the homogeneity of filler dispersion.

Polypropylene based composites containing 0.5% by volume of MWCNTs have been prepared by melt compounding and analyzed to estimate their actual level of filler dispersion. In particular, three types of commercial multi walled carbon nanotubes with the same aspect ratio and different surface features has been included in the melt under the same processing condition.

Results confirm that chemical features of the interface play a key role on the achieved filler dispersion. In our case, analytical data show a relevant improvement of the dispersion index in presence of functionalized carbon nanotubes with respect to samples containing non-functionalized ones. As displayed in Fig. 2, the density of agglomerates decreases as a function of CNT functionalization. Poorly dispersed nanotubes in the polymer matrix shows on average both the highest number and the largest size of agglomerates, producing therefore more scattering and therefore an increased interaction between the nanocomposite medium and the e.m. wave. This translates in increased  $n$  and  $\alpha$  values in the THz region.

Thus, one can conclude that the study of the e.m. interaction between a THz wave and a PP matrix loaded with different types of multi-walled carbon nanotubes can be used as a reliable and powerful tool to estimate the level of nanofillers dispersion inside the polymeric compound. Work is in progress to verify if analogous considerations can be also extended to nanocomposites containing filler with different aspect ratios and shapes and over a different range of filler contents even below the theoretical percolation threshold.

#### Acknowledgments

This work has been partially supported by the POR Campania FSE 2007-2013 through MASTRI (Materials and Smart Structures) Project. One of the authors (AA) acknowledges partial support from MPNS COST ACTION MP1204 - *TERA-MIR Radiation: Materials, Generation, Detection and Applications*. All the authors gratefully thank Dr. Alessandro Garziano and Dr. Carlo Natale (Istituto Italiano Tecnologie, Italy) for their helpful contribution on image analysis and discussion.